Large Eddy Simulation of Turbulent Swirling Flow Through a Sudden Expansion

Walter GYLLENRAM	Chalmers Univ. of Technology, Göteborg, Sweden	gyllwalt@chalmers.se
Håkan NILSSON	Chalmers Univ. of Technology, Göteborg, Sweden	hani@chalmers.se
Lars DAVIDSON	Chalmers Univ. of Technology, Göteborg, Sweden	lada@chalmers.se

Key words: Turbulence, swirl, draft tube, oscillations, vortex breakdown, LES, CFD.

Abstract

Turbulent swirling flow through a sudden expansion is investigated numerically using Large Eddy Simulation (LES). The flow resembles the flow in a draft tube of a water turbine that is working at part load. The swirling inflow is subject to a strong adverse pressure gradient and the symmetry of the flow breaks down close to the inlet. This gives rise to an oscillating, helicoidal vortex core which in turn creates a highly unsteady and turbulent flow field. In this work, the large-scale turbulent structures are numerically resolved, and detailed information about the flow characteristics is obtained. The oscillating flow is analysed using Fourier transforms of the wall pressure at different downstream locations. The most dominant frequency corresponds to the rotational rate of the precessing vortex core, and it is found that this frequency is constant throughout the domain. The results of two simulations using numerical discretization schemes of different order are compared. It is shown that the frequency of the precessing vortex core is not sensitive to the choice of discretization. However, the lower frequencies of the flow depend to a higher extent on the numerical accuracy. To validate the results, the computed velocities are averaged and compared to experimental data. The agreement is good. The Reynolds stress tensor is also computed and analysed. It is found that large degrees of turbulent anisotropy are found only in the region that is dominated by the oscillating vortex core. Further downstream, the degree of turbulent anisotropy is almost negligible despite the relatively higher level of swirl.

Introduction

Swirling flows are found in numerous technical applications, e.g. turbines, compressors, pumps, fans and combustors. The aim of the present work is to acquire an understanding of the physics of unsteady swirling flow in draft tubes of hydraulic power plants. In hydraulic power plants of a Francis or Kaplan type, the swirling flow is created in the wicket gate just upstream of the runner. The runner rotates in the same direction as the flow and the blades of the runner will counteract and neutralise the swirling velocity component if the turbine is working at its design point. However, at part load, a swirling flow will exit the runner and enter the draft tube in the

form of a large vortex. This vortex may, because of the strong adverse pressure gradient in the draft tube, break down into a precessing asymmetric shape and give rise to an oscillating pressure field. In Francis turbines, these pressure fluctuations may cause vibrations of a magnitude that endangers the supporting structure of the machine. The amplitude of the pressure fluctuations in Kaplan turbines is usually not strong enough to cause structural damage. However, the draft tube of a Kaplan turbine is very sensitive to flow separation, which can be triggered by the fluctuations. This may have a serious impact on the efficiency of the power plant. It is necessary to be able to accurately predict these features of the flow in order to improve the hydrodynamical design of the turbine. Special attention must be paid to boundary conditions and turbulence modeling of swirling flow in general. Moreover, if a swirling flow is subject to an adverse pressure gradient as in the present case, it will be even more intriguing to model accurately.

At present, steady Reynolds-Averaged Navier-Stokes (RANS) simulations are usually used for industrial CFD. Because of the rapidly increasing computer power, unsteady simulations are expected to be more common. In unsteady simulations there is a potential in resolving the large turbulent structures and observing how they interact in the flow field and with the construction. However, RANS turbulence models are calibrated for steady flow, i.e. they are usually tuned to model all turbulent time scales and consequently all turbulent length scales as well. This will in many cases cause an unsteady RANS simulation to converge to an unphysical steady solution. Large eddy simulation (LES) is regarded as a more suitable tool for accurate simulations of unsteady flow. In LES, the Navier-Stokes equations are filtered in space and the unknown terms that emanate from the non-linearity of the equations are considered subgrid turbulence. Hence the upper limit of the length scales of the modeled turbulence is proportional to the local grid resolution, and information about the large turbulent scales is found in the solution of the flow field. Beside the inability of many RANS turbulence models (i.e. eddy-viscosity models) to work properly in unsteady simulations, another shortcoming is their tendency to underpredict the high levels of turbulent anisotropy that are often found in swirling flow. The high levels of turbulent anisotropy are not a problem in a well-resolved LES. Even though the subgrid turbulence model that is usually used in LES is much simpler than a RANS eddy-viscosity model, most of the anisotropic turbulent scales are resolved and simply need not be modeled.

In this paper, the unsteadiness and structure of a post-breakdown swirling flow is examined by LES in order to obtain new and detailed information on the structure of the vortex core and turbulence. The case that was chosen for the present study has earlier been examined experimentally by Dellenback et al. (Ref 1) It is a swirling flow through a sudden expansion (Fig. 1) at a Reynolds number of $40,000$ based on the inlet diameter and bulk velocity. The experimental data have been used to define the inlet boundary conditions and to validate the numerical solution. Earlier numerical investigations of the present case have been made by Schlüter (Ref 2, 3) and Schlüter et al. (Ref 4) In these papers there is no information on unsteady behaviour of the flow, but the importance of using unsteady inlet boundary conditions for low swirl numbers is demonstrated in the paper by Schlüter et al. (Ref 2) There is most likely a need for unsteady turbulent inlet boundary conditions for small swirl numbers because the wall normal turbulent mixing is underpredicted if steady inlet boundary conditions are used. However, for the high swirl number that is considered in the present case, there is no significant difference in the time-averaged results irrespective of whether the boundary conditions are steady or not. In the present work, the same case was simulated using two different numerical discretization schemes. The unsteadiness of the flow is analysed by Fourier transforms of wall pressure. It is shown that the main (rotational) frequency of the precessing vortex core is not sensitive to the

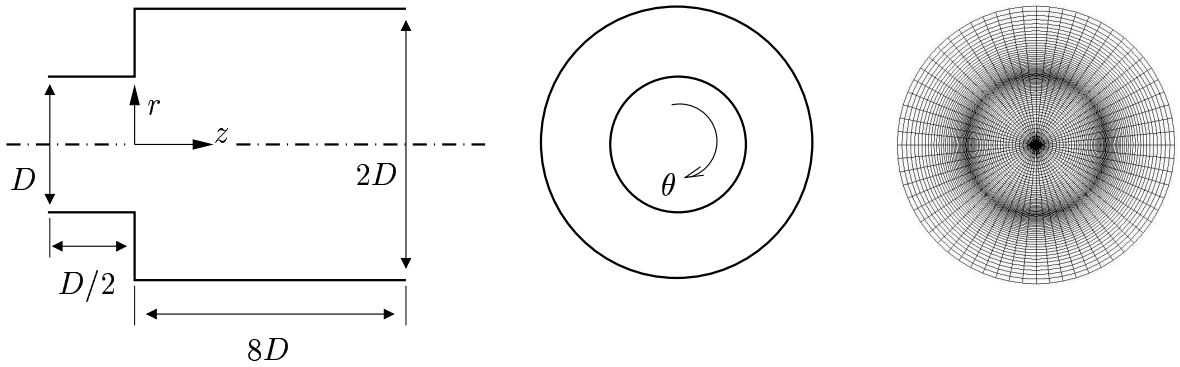

Figure 1 Geometry of the test case (left, center) and cross-section of the computational grid (right).

numerical accuracy. However, there are lower frequencies of the flow that are more sensitive. The computational results are averaged in time as well as in the azimuthal (homogeneous) direction in order to render a comparison with experimental data possible. The Reynolds stress tensor for the averaged velocity field is also computed from the instantaneous results, and it is also shown that the precessing vortex core itself is the mother of most turbulent anisotropy of the flow.

Method

The CALC-PMB (Ref 5) CFD software was used for the calculations in this work. CALC-PMB was developed at the Division of Fluid Dynamics, Department of Applied Mechanics at Chalmers University of Technology, Gothenburg. It is based on the finite volume method, and the pressure-velocity coupling is solved using the SIMPLEC algorithm developed by van Doormaal (Ref 6). Conformal block-structured, boundary-fitted coordinates are used, and the code is parallelized by domain decomposition.

A computational mesh of $1,500,000$ nodes was created for the present numerical investigations. The domain was decomposed into 15 blocks for parallel distribution. The computational grid is similiar in cell distribution and size to the grid used by Schlüter (Ref 2, 3) and Schlüter et al. (Ref 4), see Fig. 1. The time step was chosen to assure a CFL number smaller than one in all cells. The computations were considered to be converged when all normalised residuals were of the order of 10^{-3} in each time step. The residuals of the momentum equations were normalised with the corresponding convection, and the continuity error was normalised with the mass flow rate. The Smagorinsky turbulence model was used for the subgrid turbulent length scales.

The geometry and the grid were generated in the ICEM CFD/CAE commercial software. For post-processing, the Matlab and Ensight commercial softwares were employed.

Boundary conditions

The inlet boundary condition for the mean velocities was constructed by spline curves based on the measured data. A boundary layer based on the log-law was added between the (radially) outermost measuring point and the wall. As mentioned in the introduction, earlier investigations of the same case by Schlüter et al. (Ref 4) showed that the turbulence level of the inlet boundary conditions has large effects on the mean velocity profiles if the swirl level is low. However, in the present study, the swirl level is high enough for a fast transition to turbulence and there

is no need to add unsteadiness at the steady inlet boundary condition. The common kinematic (non-porous walls) and viscous (no slip) conditions were used at the walls. The convective outlet boundary condition $\partial_0 U_i + U_z \partial_z U_i = 0$ was implemented instead of the more common $\partial_0 U_i + \overline{U} \partial_z U_i = 0$, where z denotes the axial direction and $\overline{U}$ is the average axial velocity through the outlet cross-section. The former is a true convective formulation that will take into account the boundary layer and wake regions of the flow.

Results and discussion

A swirling flow may under certain conditions undergo vortex breakdown, i.e. a sudden change of flow structure that is sometimes connected to local flow reversal along the centerline. In this case the result of the vortex breakdown is a precessing helicoidal vortex core (see Fig. 2), and the motion of this structure gives rise to an oscillating pressure field. The precessing vortex core is located in a region between the sudden expansion and a point approximately one and a half diameters downstream.

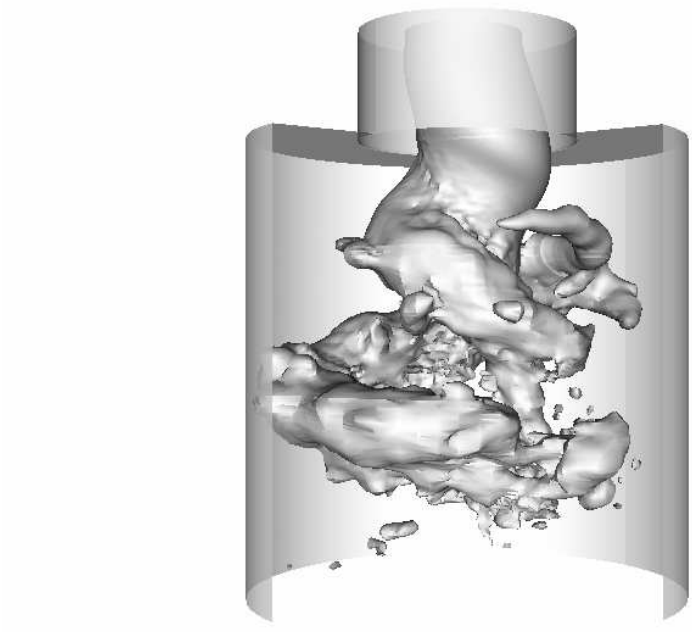

Figure 2 Snapshot of the precessing vortex core visualised by an iso-surface of the static pressure. The helicoidal vortex structure is formed immediately after the expansion. It dominates the flow until a point approximately one and a half diameters downstream of where it is formed.

Mean velocity

The velocity and Reynolds stress profiles that are presented in this paper were averaged in time as well as in the tangential direction in order to save CPU hours. The averaged velocity profiles are shown in Fig. 3. They agree well with the experimental data. A strong recirculation zone is formed around the centerline just downstream of the sudden expansion in Fig. 3 (top left). However, the calculated magnitudes of the reversed velocities are somewhat overpredicted in this region compared to the experimental data. The difference in the results from using the van Leer and the second-order central difference scheme is most obvious near the wall where the gradients are very high. Further downstream, the results obtained by using the central difference

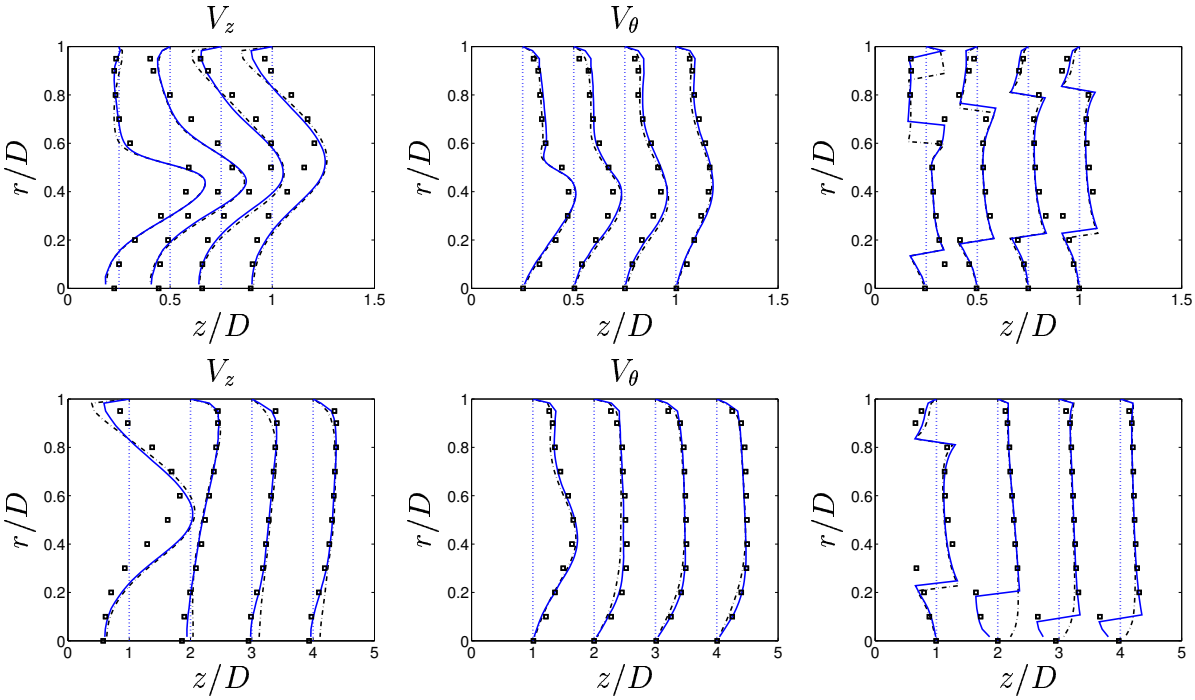

Figure 3 Radial distributions of averaged axial velocity (left column), tangential velocity (center column) and swirlangle (right column) at different cross-sections. [$\cdot-$]: van Leer scheme. [$-$]: Central difference scheme. [$\square$]: Experiment. The largest differences between the two schemes are seen in the near-wall behaviour, and only the central difference scheme will accurately predict the downstream evolution of the recirculation zone around the symmetry axis. The scaling between the top and bottom rows is given by the profiles at $z/D = 1$. The difference between the two schemes in predicting the downstream evolution of the recirculation zone is clearly visible from the sign of the swirl angle. The van Leer scheme fails to predict the width of the recirculation zone, but very good results are obtained using the central difference scheme.

scheme correspond very well to experimental data. The lower-order van Leer scheme is obviously not accurate enough to predict the downstream evolution of the near-wall boundary layer on this grid. As also shown in Fig. 3 (bottom left), the recirculation along the centerline vanishes when the van Leer scheme is employed. This is of course connected to the underprediction of the velocities in the boundary layer simply by the fulfilment of the continuity constraint. The tangential velocity profiles correspond better to the experimental data than the axial velocity profiles. The differences between the results from using the van Leer and the central difference schemes are also smaller for the tangential component. An analysis of the swirl angles yields local information about the combination of axial and tangential velocity components. Small differences in the velocity profiles can give rise to large differences in swirl angles. The downstream evolution of the relation between the tangential and axial velocities, i.e. $\arctan\left(V_\theta/V_z\right)$, is shown in the right column of Fig. 3. A negative value corresponds to a region of reversed flow since $V_\theta \geqslant 0$ everywhere. Very good agreement with experimental data is obtained by employing the central difference scheme. Discrepancies between the experiments and the calculations using the central difference scheme are found only at the regions that correspond to the beginning ($z/D \approx 0.25$) and the end ($z/D \approx 1$) of the helicoidal vortex structure shown in Fig. 2.

The largest differences between the numerical and the experimental results seem to be concentrated in the region close to the inlet. If the inlet boundary conditions were located further upstream, it is very likely that the precessing motion of the velocity field would propagate up-

stream until it reaches this location. The higher degree of freedom near the sudden expansion would of course influence the axial velocity profile. The precessing motion of the velocity field would make the time-averaged axial velocity profile look smoother, i.e. the region of reversed flow along the centerline would be extended radially. This would probably cause the reattachment length to be shorter, and the computed results would correspond even better to the experimental data. From the observation of the overprediction of reversed near wall flow in Fig. 3 (top left) it is tempting to assume that the helicoidal vortex structure that is computed in this work breaks down at a point further downstream of where it did in the experiments, especially when using the van Leer scheme. The results from the simulation using the van Leer scheme especially overpredict the reversed near-wall flow in a way that is far from satisfying. This could also be rectified by moving the inlet boundary condition further upstream. For a more detailed analysis, see Gyllenram (Ref 7).

Turbulence

The Reynolds stresses of the flow are computed by subtracting the averaged velocity field from the instantaneous data. In this section, the results for $z/D \geqslant 2$ have been multiplied by a factor of two in order to make the figures more clear. The computed normal, tangential and axial Reynolds stresses are compared to experimental data in Fig. 4. The agreement is quite good, especially for the simulations using the central difference scheme. The very sharp peak of $\overline{v_z' v_z'}$ at $z/D = 0.25$ (Fig. 4, top left) was not captured by the measurements, probably because of the choice of measuring points. The computed normal stresses are slightly overpredicted further downstream at $z/D = 2$ (Fig. 4, bottom left) . This is a location just downstream of where the helicoidal vortex structure breaks down. As already mentioned in the previous section, it is likely that the simulations predict a helicoidal vortex structure that is stretched just a little bit too far in the axial direction. This would slightly displace the point at which this structure breaks down into turbulence and explain why the turbulent normal stresses are overpredicted at

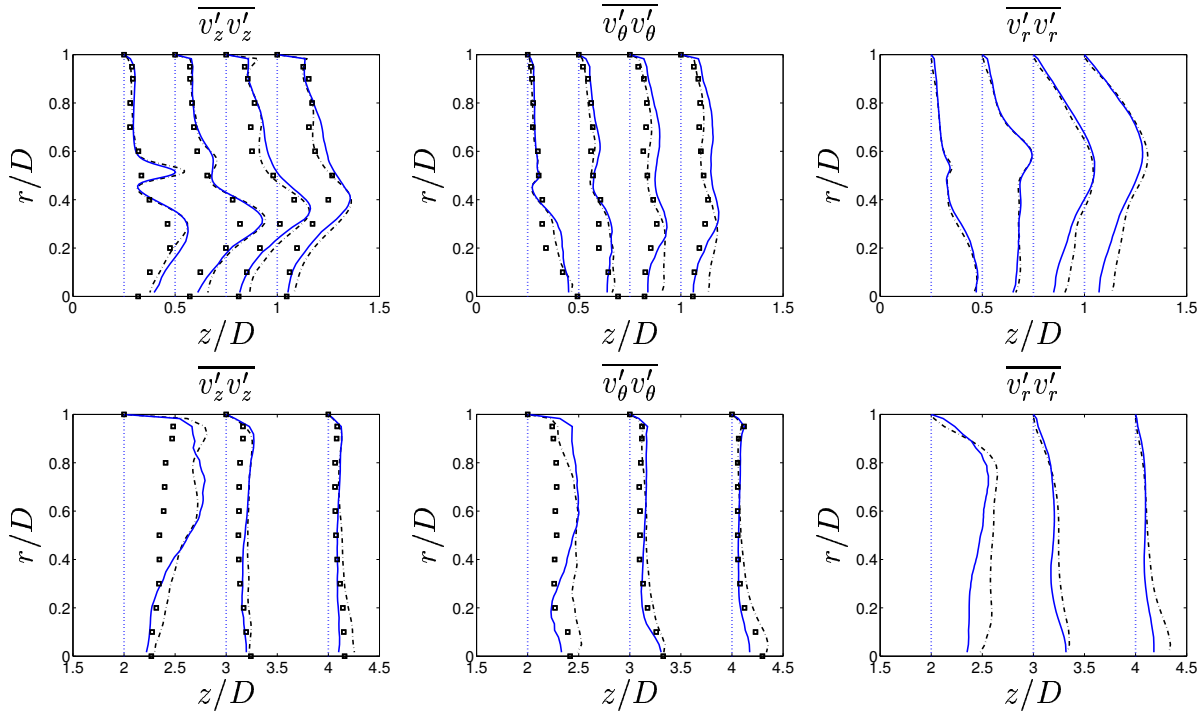

Figure 4 Radial distribution of normal Reynolds stresses. [$\cdot-$]: van Leer scheme. [$-$]: Central difference scheme. [$\square$]: Experiment. The data presented in the bottom row have been multiplied by a factor of two.

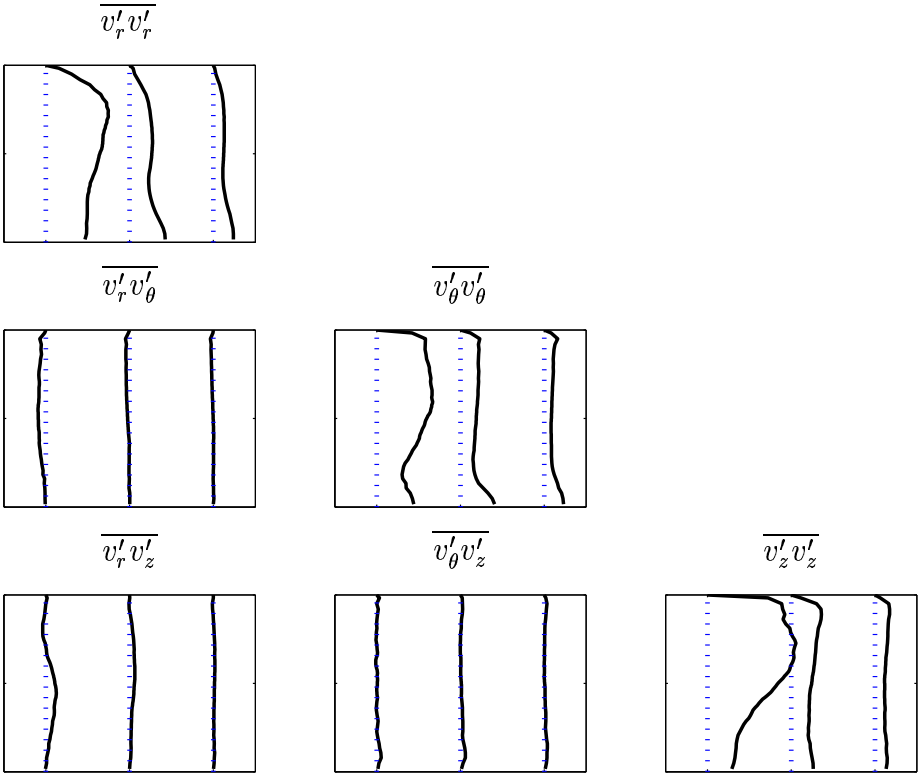

Figure 5 Radial distribution of $\overline{v_i'v_j'}$ at downstream positions $z/D = 2,\ 3$ and 4. The central difference scheme was used. The precessing vortex core creates a high degree of turbulent anisotropy at the entrance to the expansion. Further downstream, the anisotropy is not very significant despite the high swirl number of $S^* > 0.8$.

$z/D = 2$, especially by the simulation using the van Leer scheme.

The high level of anisotropy of the turbulence of swirling flows is often considered one the most difficult properties to model accurately. However, the streamwise evolution of the Reynolds stress tensor (Fig. 5) suggests that, in this case, the anisotropy is not significant. The only region where the anisotropy can be considered high is at the very entrance to the expansion, i.e at $(r/D,\ z/D) = (0.5,\ 0.25)$. Despite the very high swirl number, $S^* > 0.8$, at the downstream cross-sections, the anisotropy is still very low. As the region of high anisotropy is completely dominated by the precessing vortex core, there is clearly a potential in resolving this structure in space and time and using simple models for the non-resolved turbulence.

Swirl levels

A swirl number must be defined in order to obtain a global measure of the swirl level of a swirling flow. The most common choice is to relate the flux of angular momentum to the flux of axial momentum according to

$$S = \frac{\int_0^R V_\theta V_z\, r^2\, dr}{R \int_0^R V_z^2\, r\, dr}. \tag{1}$$

However, this definition is not a good choice for recirculating flow. The definition will give a lower swirl number for a given tangential velocity profile when a recirculation zone is developing along the centerline as compared to a non-recirculating flow. Because of the square in the nominator, only the integrand in the denominator will change sign when backflow occurs. For

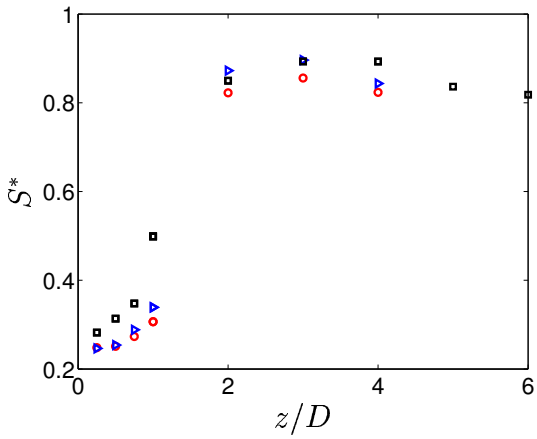

Figure 6 Downstream evolution of the swirl number, S^*. [○]: van Leer scheme. [▷]: Central difference scheme. [□]: Experiment. At the inlet of the computational domain, the swirl number is $S^* = 0.6$ and there must obviously be a strong decrease in swirl number before the sudden expansion at $z/D = 0$ is reached.

the present study a more general definition is proposed,

$$S^* = \frac{\int_0^R |V_\theta| V_z \, r^2 \, dr}{R \int_0^R |V_z| V_z \, r \, dr}. \tag{2}$$

By this definition, the direction of the flux will also have an influence in the nominator. The downstream evolution of the swirl number, S^*, is shown in Fig. 6. Since the swirl number at the inlet ($z/D = -1$) is $S^* = 0.6$, there is a rapid decrease of this parameter as the flow approaches the sudden expansion. This is explained by the rapid deceleration of the axial velocity along the centerline, which must lead to accelerated axial velocities in the boundary layer. However, as the axial velocity rapidly decreases just downstream of the sudden expansion, there is consequently an increase in swirl number until the flow reattaches and the tangential boundary layer starts to develop, see Fig. 3. At this point, the axial velocity profile becomes smoother and a natural decay of swirl is induced by wall friction.

Frequencies of the flow

The mean characteristic frequencies of the flow are obtained by averaging a group of ten Fourier transforms of time series of wall pressure that are each $12,000$ time steps in length. The time series overlap each other by $9,000$ time steps, and each series corresponds to 0.144 seconds of real time or, as it would turn out, approximately 26 revolutions of the vortex rope. This procedure is used in order to avoid oscillations in the frequency spectra. The spectral power density of the wall pressure is shown in Fig. 7. It is clear that the most dominant frequency in the spectrum is at a Strouhal number ($St = f \times D/U_{bulk}$) of approximately 0.64. This value corresponds to the motion of the precessing vortex core and is obviously not sensitive to the choice of disctretization scheme. However, as shown in Fig. 7, there are lower frequencies of the flow that are definitely sensitive to the choice of scheme. The distinct frequency at $St = 0.2$ is not found in the case using the van Leer scheme but is present throughout the domain in the case using the central difference scheme, except for the region around $z/D = 1$ where the peak vanishes under the influence of randomly distributed lower frequencies. The fact that the lower peak of spectral density of the pressure frequencies obtained when using the van Leer scheme is not present at any point means that the lower frequencies in this case have a higher degree of

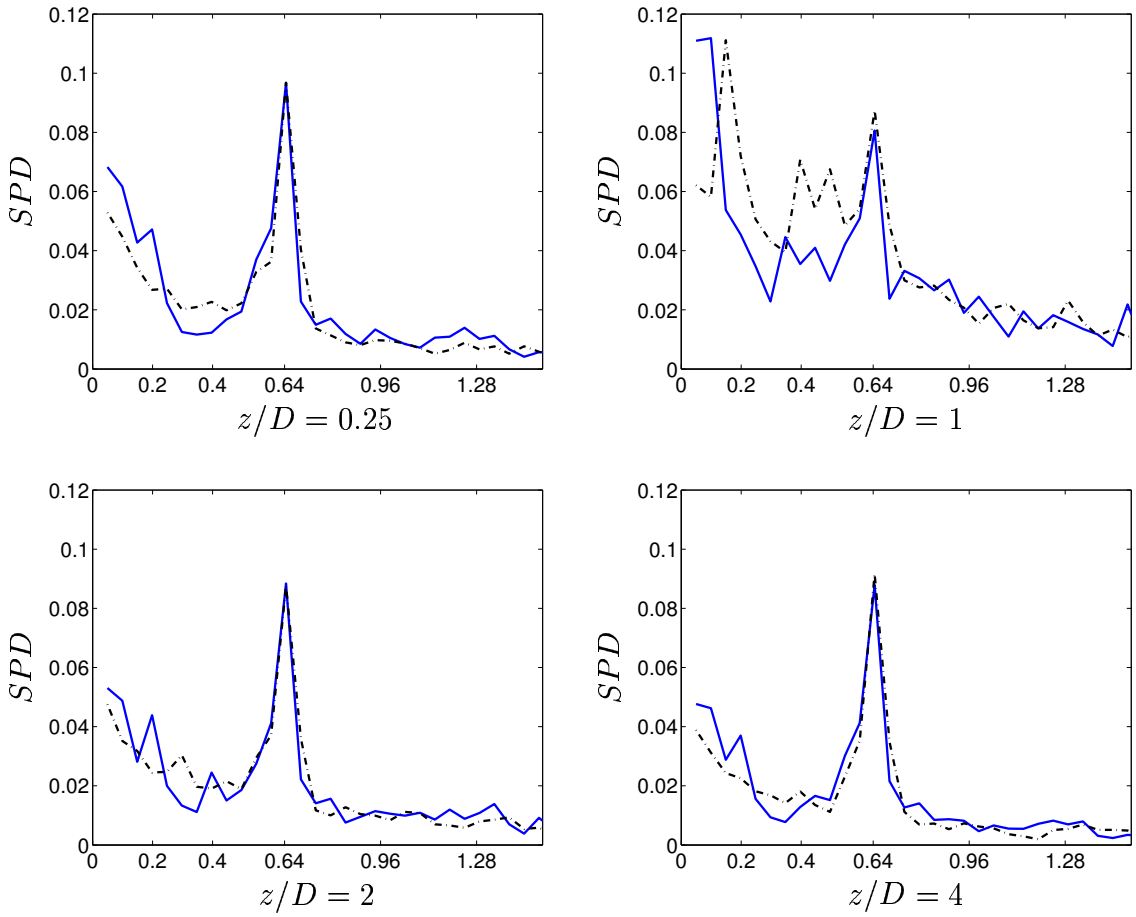

Figure 7 Spectral power density of wall pressure as a function of Strouhal number. [$\cdot-$]: van Leer scheme. [$-$]: Central difference scheme. The most dominant frequency is at Strouhal number $St = f \times D/U_{bulk} = 0.64$. This frequency corresponds to the rotation of the vortex core.

randomness. The ability to capture distinct lower frequencies is obviously a numerical issue.

Figure 7 shows that the density of lower frequencies increases around $z/D = 1$, where the helicoidal vortex structure breaks up into turbulence and a more symmetric vortex structure evolves. These lower frequencies may be related to the vortices of the separation zone. In this region, large vortices build up and roll down along the wall under the influence of the precessing vortex. Since the spread of the separation zone is the main dicrepancy between the two simulations, the discrepancy between the obtained frequencies may reflect the motion of the large vortices. Further downstream of the breakdown of the helicoidal vortex structure, the spectral density at high frequencies decays because of relaminarisation of the turbulence.

Conclusions

A swirling flow through a sudden expansion was studied using LES. The results of two simulations using two different discretization schemes are compared to experimental data. Good results are obtained when the second-order central difference scheme is used.

It is shown that the frequency of the precessing vortex core is not sensitive to the choice of discretizing scheme. However, lower frequencies are present in the spectrum that will in fact be influenced by the numerical accuracy. These frequencies are amplified at an axial position near the point at which the helicoidal vortex structure breaks up into turbulence and a more symmet-

ric vortex structure evolves. At this point, the turbulence level also increases. In order to catch the periodicity of the lower frequencies, high order numerical schemes (or very well resolved computational grids) must be used. This is somewhat surprising because one would intuitively expect the higher frequencies to depend more on the numerical scheme and resolution.

The largest discrepancies between the experiment and the calculations are located at a position near the sudden expansion where the flow is dominated by the precessing vortex core. If the precessing motion of the vortex core had been allowed to propagate further upstream, the discrepancies between the computed and experimental results would have been smaller. Hence, if a steady inlet boundary conditions is used, it is important to make a careful consideration of the location of the inlet of the computational domain if a precessing vortex core is expected to be a part of the solution.

It is also shown that the inability of many RANS eddy-viscosity models to predict a high level of anisotropy can not be the main reason for the failure of these models in swirling flow. High levels of turbulent anisotropy in this case are only found at the entrance to the expansion, where the flow is completely dominated by the precessing vortex core. Further downstream, the level of turbulent anisotropy is still very low despite the relatively higher swirl number. Since the region of high anisotropy is dominated by the precessing vortex core, there is obviously a potential in resolving this structure and using simple models for the small-scale turbulence.

Acknowledgements

The research presented in this paper has been part of the "Water turbine collaborative R&D program", which is financed by the Swedish Energy Agency, Hydro Power companies[1] (through Elforsk AB), GE Energy (Sweden) AB and Waplans Mekaniska Verkstad AB.

References

Ref 1 P.A Dellenback, D.E. Metzger, and G.P. Neitzel. Measurements in turbulent swirling flow through an abrupt expansion. *AIAA Journal*, 26:6:669–681, 1987.

Ref 2 J. U. Schlüter. Consistent boundary conditions for integrated RANS/LES computations: LES inflow conditions. In *16th AIAA CFD Conference*, volume AIAA-2003-3971, 2003.

Ref 3 J. U. Schlüter. Influence of axisymmetric assumptions on large eddy simulations of a confined jet and a swirl flow. *International Journal of Computational Fluid Dynamics*, 18(3):235–246, 2004.

Ref 4 J. U. Schlüter, H. Pitsch, and P. Moin. Large eddy simulation inflow conditions for coupling with Reynolds-averaged flow solvers. *AIAA Journal*, 42(3):478–484, 2004.

Ref 5 H. Nilsson. *Numerical Investigations of Turbulent Flow in Water Turbines*. Thesis for the degree of Doctor of Philosophy, ISBN 91-7291-187-5, Chalmers University of Technology, Göteborg, Sweden, 2002.

Ref 6 J.P. Van Doormaal and G.D. Raithby. Enhancements of the SIMPLE method for predicting incompressible fluid flows. *Num. Heat Transfer*, 7:147–163, 1984.

Ref 7 W. Gyllenram. *Analytical and Numerical Investigations of Steady and Unsteady Turbulent Swirling Flow in Diffusers*. Thesis for the degree of Licentiate of Engineering, no. 2006:05, ISSN 1652-8565, Chalmers University of Technology, Göteborg, Sweden, 2006.

[1] Vattenfall AB Vattenkraft, Fortum Generation AB, Sydkraft Vattenkraft AB, Skellefteå Kraft AB, Graninge Kraft AB, Jämtkraft AB, Sollefteåforsens AB, Karlstads Energi AB, Gävle Energi AB, Öresundskraft AB